CHEMICAL ENGINEERING TRANSACTIONS
VOL. 46, 2015
A publication of AIDIC
The Italian Association of Chemical Engineering
Online at www.aidic.it/cet
Guest Editors: Peiyu Ren, Yancang Li, Huiping Song

**ISBN** 978-88-95608-37-2; **ISSN** 2283-9216
DOI: 10.3303/CET1546183

# Mechanics Property Analysis of High-resistance Steel Wire Mesh in Slope Flexible Stabilization System

Gaosheng Wang*, Shaoqing Shi, Min Wang

Department of Civil Engineering, Logistical Engineering University, Chongqing, China.
hdwanggaosheng@163.com

This paper aims at studying deformation mechanism and mechanics property of high-resistance steel wire mesh in slope flexible stabilization system and makes theoretical analysis under unilateral tension, and the analytical results are compared with the FEM and experimental results. It makes it uncovered that shape parameters of high-resistance steel wire mesh effect towards deformation mechanism and mechanics property; Above results provide a technical reference for engineering application.

## 1. Introduction

Slope flexible stabilization system refers to strengthen potential disasters of slope surface by flexible net (steel cable mesh, steel wire mesh), which has notable technical and economic advantages and environmental protection advantages compared with traditional slope rigid stabilization system represented by sprayed concrete, mortar rubble, etc. (Shi, Wang and Sun (2013); Yang and Zhou (2006); Wang and Shi (2011); Bertolo, Oggeri and Peila (2009); Yang, Zhou and Jiang (2005); Daniel and Luis (2009)).
In recent years, the use of GTC flexible stabilization system (as shown in Figure 1) is becoming increasingly wider, as a new kind flexible stabilization system with better resistance against creep deformation. The engineering practices show that GTC flexible stabilization system can replace the traditional flexible stabilization system (Luo, Lei and Zhou (2006); Shi, Wang, Peng and Yang (2013); Díaz and Nieto (2009)) in a more economical way under the circumstances that protection function and capacity needs are guaranteed. GTC flexible stabilization system is mainly made up by the high-resistance steel wire mesh weaved by high-resistance steel wire. It has the characteristics of high-resistance, easy to stretch, corrosion resistance. Yang (2006) and some experts (He, Peng and Yang (2006); Xiang, He and Ouyang (2014)) introduce the basic working principle and characters, and J.J. del Coz Díaz (2009) makes FEM and experiment of high-resistance steel wire mesh under unilateral tension, however, high-resistance steel wire mesh in the field of GTC flexible stabilization system mainly focus on specific applied experiment(Díaz and Nieto (2009)) instead of in-depth study of basic theory, design and calculation method, which has influence on the application of high-resistance steel wire mesh in the field of GTC flexible stabilization system.
This paper, simplifying the force towards high-resistance steel wire mesh to uniform load, analyses its deformation mechanism and mechanics property, and the analytical results are compared with the FEM and experimental results.

## 2. Deformation Mechanism of High-resistance Steel Wire Mesh

High-resistance steel wire mesh is made up of special steel wire mesh with high-resistance, easy to stretch and solid surface. It is a type of mesh weaved by diamond-shaped net hole without bonding which can realize optimal transmit under the external forces through adaptive adjustment linked by special steel wires and avoid overstress in part. The deformation capacity of GTC flexible stabilization system is rested with deformation capacity of high-resistance steel wire mesh.
Deformation capacity of high-resistance steel wire mesh depends on the shape and size of high-resistance steel wire mesh unit. The shape and size of unit applied in this paper are as shown in Figure 3. The length of

Please cite this article as: Wang G.S., Shi S.Q., Wang M., 2015, Mechanics property analysis of high-resistance steel wire mesh in slope flexible stabilization system, Chemical Engineering Transactions, 46, 1093-1098 DOI:10.3303/CET1546183

slanted side of the unit cell is $l$, and the diameter $d$, the angle $\theta$ ($0<\theta<\pi/2$), elasticity modulus of special steel wire $E_S$

*Figure 1: GTC flexible stabilization system*

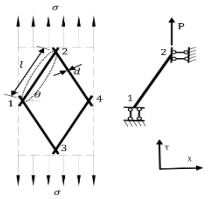

*Figure 2: The force diagram of high-resistance steel wire mesh unit in the Y direction*

The diameter $d$ of high-resistance steel wire mesh unit wall is short compared with the length of slanted side $l$. Beam theory can be applied to analyze the deformation mechanism of high-resistance steel wire mesh (Lorna and Michael (1999)). Make use of symmetry of high-resistance steel wire mesh unit to choose feature shape as shown in Figure 2, when uniform stretching stress in the Y direction is $\sigma$, the component force in the X direction is required to be 0 by balance condition and deformable coordination condition. Point 1 and 2 which tend to make the unit wall bended suffer from the equal moment $\mathrm{M}$ and tension $P$.
In analyzing the unit wall 1-2 of Figure 2, it can be learned from static equilibrium:

$$\mathrm{P}=\sigma l\cos\theta\cdot d \tag{1}$$

$$\mathrm{M}=\frac{\mathrm{P}l\cos\theta}{2} \tag{2}$$

From standard beam theory, the bending deflection is:

$$\delta=\frac{\mathrm{P}l^3\cos\theta}{12\mathrm{E}_s\cdot\mathrm{I}} \tag{3}$$

$\mathrm{I}$ in the formula means sectional inertia moment (for circular sectional unit wall, $\mathrm{I}=\pi d^4/64$).
If sheer load on the wall 1-2 is $\mathrm{P}\cos\theta$, sheer deflection is:

$$\delta_s=\kappa\frac{\mathrm{P}l\cos\theta}{GA} \tag{4}$$

For circular cross section, $\kappa=10/9, A=\pi d^2/4$; $G$ refers to shear elasticity, and $G=\mathrm{E}_s/2(1+\nu)$ ($\nu$ means Poisson ratio of special steel wire).
Axial load on wall of hold is $\mathrm{P}\sin\theta$, so axial deflection is:

$$\delta_{\mathrm{a}}=\frac{\mathrm{P}l\sin\theta}{\mathrm{E}_sA} \tag{5}$$

Therefore, total deflection in the Y direction is：

$$\delta_Y=\frac{\mathrm{P}l^3\cos\theta}{12\mathrm{E}_s\cdot\mathrm{I}}\cos\theta+\kappa\frac{\mathrm{P}l\cos\theta}{GA}\cos\theta+\frac{\mathrm{P}l\sin\theta}{\mathrm{E}_sA}\sin\theta$$

$$=\frac{\mathrm{P}l^3}{\pi\mathrm{E}_s\cdot d^4}\left[\frac{16}{3}\cos^2\theta+\frac{80(1+\nu)}{9}\left(\frac{d}{l}\right)^2\cos^2\theta+4\sin^2\theta\cdot\left(\frac{d}{l}\right)^2\right] \tag{6}$$

In the formula,

$$g_Y(\theta,\beta)=\left(\frac{16}{3}+\frac{80(1+\nu)}{9}\beta^2\right)\cos^2\theta+4\sin^2\theta\cdot\beta^2 \tag{7}$$

$\beta=d/l$ refers to the ratio of sectional diameter and length of the unit slanted wall.
The equivalent strain of high-resistance steel wire mesh unit in the direction of Y should be:

$$\varepsilon_Y=\frac{\mathrm{P}l^2\cdot g_Y(\theta,\beta)}{64\mathrm{E}_s\cdot\mathrm{I}\cdot\sin\theta} \tag{8}$$

If the pull rod acting force in the direction of length of unit wall is N, the compound normal stress of max bending stresses and tension stresses of the peripheral point in the direction of sheer in Point 1(or 2)'s circular section is:

$$\sigma_{\max} = \frac{\mathrm{P}d}{4 \cdot \mathrm{I}}\left( l\cos\theta + \frac{d\sin\theta}{4} \right) \tag{9}$$

Then, the max normal strain is:

$$\varepsilon_{\max} = \frac{\mathrm{P}d}{4\mathrm{E}_s \cdot \mathrm{I}}\left( l\cos\theta + \frac{d\sin\theta}{4} \right) \tag{10}$$

Consequently, strain amplification coefficient defines as:

$$R(\theta,\beta) = \frac{\varepsilon_Y}{\varepsilon_{\max}} \tag{11}$$

When $\beta$ small, axial deformation and sheer deformation caused by unit wall is can be ignored compared with bending deflection. Simplified formula (11):

$$g_Y(\theta,\beta) = \frac{\cot\theta}{3\beta} \tag{12}$$

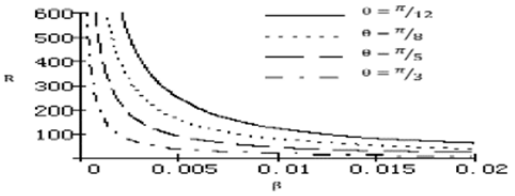


*Figure 3: Changing curves of strain amplification coefficient $R$ over $\beta$*

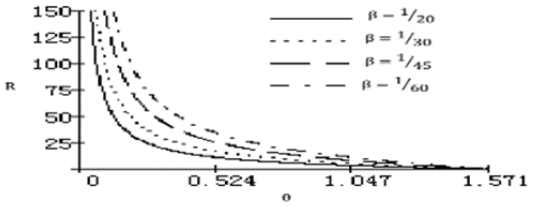


*Figure 4: Changing curves of strain amplification coefficient $R$ over angle $\beta$*

The reference (Díaz and Nieto (2009)) gives a uniaxial resistance test of $1000\times1000mm$ high-resistance steel wire mesh (dimension unit size $83\times143mm$ , $d = 3mm$ , $\sigma_s = 1770MPa$ ), and its maximum deformation is 60 mm in Simple Tension. The corresponding parameters are into formulas (10), (11) and (12), when $\sigma_{\max} = \sigma_t = 1.25\sigma_s$ , getting that R is 5.332 and deformation is 56.176 mm. It illustrates the rationality of the paper's analysis involving deformation mechanism of high-resistance steel wire mesh. Strain amplification coefficient is only concerned with $\theta$ and $\beta$ from the formula (11) and (12), and changing curves of strain amplification coefficient $R$ over $\beta$ and angle $\theta$ are demonstrated in Figure 3 and 4. It can be seen from Figure 3 and 4 that the deformability in the direction of Y reduces as $\beta$ enlarges; the deformability of high-resistance steel wire mesh in the direction of Y reduces as angle $\theta$ enlarges; $\beta$ has a greater influence on strain amplification $R$ coefficient from the comparison of these changing curves.

## 3. Mechanical Property of High-resistance Steel Wire Mesh

Strain in the direction of X-axis:

$$E_Y^* = \frac{\sigma}{\varepsilon_Y} \tag{13}$$

### 3.1 In-plane load

The structural shape and size of high-resistance steel wire mesh unit decides its in-plane mechanical property, and equivalent elastic modulus is often used to represent mechanical property of engineering structure(Zhang, Zhou and Qiu (2013); Wang, Shi, Yang (2014); Murray, Gandhi and Bakis (2010)).
Elasticity modulus of unit in the direction of Y as shown in Figure 2 is:
Adding above formula with formula (7) and (8):

$$E_Y^* = E_s\beta^3\frac{\pi\tan\theta}{g_Y(\theta,\beta)} \tag{14}$$

$$\varepsilon_X = \frac{\mathrm{Pl}^2 \cdot g_X(\theta,\beta)}{64\mathrm{E}_s \cdot \mathrm{I}} \tag{15}$$

In the formula,

$$g_X(\theta,\beta) = \left(4\beta^2 - \frac{16}{3} - \frac{80(1+\nu)}{9}\beta^2\right)\sin\theta \tag{16}$$

So

$$\nu^*_{YX} = -\frac{g_X(\theta,\beta)}{g_Y(\theta,\beta)}\sin\theta \tag{17}$$

Similarly, when loading in the direction of X:

$$E^*_X = E_s\beta^3 \frac{\pi\cot\theta}{g_Y(\frac{\pi}{2}-\theta,\beta)} \tag{18}$$

$$\nu^*_{XY} = -\frac{g_X(\frac{\pi}{2}-\theta,\beta)}{g_Y(\frac{\pi}{2}-\theta,\beta)}\cos\theta \tag{19}$$

Maxwell formula $E^*_Y\nu^*_{YX} = E^*_X\nu^*_{YX}$ still can be applied which shows that in plane of high-resistance steel wire mesh generally has orthogonal anisotropic. Axial deformation and sheer deformation produced by unit wall can be ignored compared with bending deflection when $\beta$ is a small number. It can be conclude that:

$$\frac{E^*_Y}{E_s} = \frac{3\pi}{16}\beta^3\frac{\sin\theta}{\cos^3\theta} \tag{20}$$

$$\frac{E^*_X}{E_s} = \frac{3\pi}{16}\beta^3\frac{\cos\theta}{\sin^3\theta} \tag{21}$$

$$\nu^*_{YX} = \tan^2\theta \tag{22}$$

$$\nu^*_{XY} = \cot^2\theta \tag{23}$$

$$E^*_Y\nu^*_{XY} = E^*_X\nu^*_{YX} = \frac{3\pi}{16}\beta^3\frac{E_s}{\sin\theta\cos\theta} \tag{24}$$

Therefore, 3 moduli are independent among $E^*_Y$, $\nu^*_{XY}$, $E^*_X$, $\nu^*_{YX}$. After convering the results of the paper's analysis involving equivalent elastic modulus, comparing them with the results of FEM and experimental test in the reference (Díaz and Nieto (2009)), and the table 1 shows the comparing results.

*Table 1: In-plane equivalent elastic modulus*

| equivalent elastic modulus | theoretical analysis | experimental test(Díaz and Nieto (2009)) | FEM(Díaz and Nieto (2009)) |
|---|---|---|---|
| $E^*_Y(KN/m)$ | 1880.95 | 1886.3 | 1690.6 |
| $E^*_X(KN/m)$ | 213.45 | 222.47 | 319.9 |

It can be seen from Table 1 that theoretical analysis results are basically consistent with the results of experimental test, which shows that theoretical analysis of mechanical property for high-resistance steel wire mesh is reasonable and right.

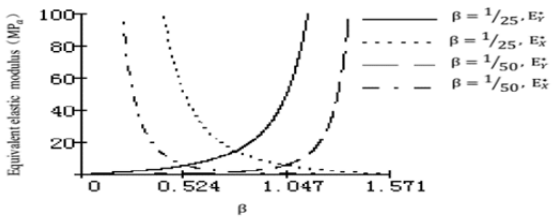


*Figure 5: Changing curves on in-plane equivalent elastic modulus over angle* $\theta$

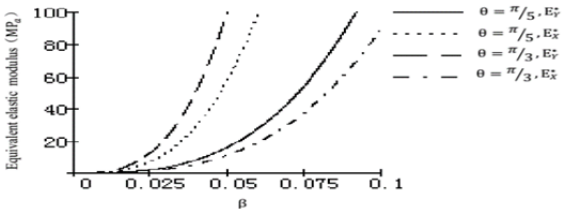


*Figure 6: Changing curves on in-plane equivalent elastic modulus over* $\beta$

Figure 5 and 6 reflect the changing on in-plane equivalent elastic modulus of high-resistance steel wire mesh over angle $\theta$ and $\beta$. It can be learned from figure 5 that as the angle $\theta$ increases, the equivalent elastic modulus in the direction of Y gradually increases, but the equivalent elastic modulus in the direction of X gradually decreases, when $\theta = \pi/4$ and $E_Y^* = E_X^*$, in-plane direction of high-resistance steel wire mesh is manifested as isotropy; It can be learned from figure 6 that the equivalent elastic modulus in the direction of X and Y increase as the $\beta$ increases; It can be learned from the comparison between Figure 6 and Figure 7 that $\beta$ has greater effect upon in-plane elastic modulus than $\theta$.

### 3.2 Out-of-plane load

When high-resistance steel wire mesh suffering from the stress of rock, soil and soil-like material in the out-of-plane vertical direction, the bearing capacity need to be considered in the out-of-plane vertical direction. If the uniform equivalent pressure stress which is parallel to Z-axis is $\sigma_s^*$, the stress F of unit's Z-direction is:

$$F = 4\sigma_s^* l^2 \sin\theta\cos\theta \tag{25}$$

Equivalent pressure strain of unit in the direction of Z is:

$$\varepsilon_z^* = \frac{F}{E_S 2ld} \tag{26}$$

Equivalent elastic modulus in the direction of Z can be defined as:

$$E_z^* = \frac{\sigma_Z^*}{\varepsilon_Z^*} \tag{27}$$

Adding formula (25), (26) and (27):

$$E_z^* = \beta\frac{E_S}{\sin 2\theta} \tag{28}$$

## 4. Conclusions

The following results can be got from the analysis on deformation mechanism and mechanical property of high-resistance steel wire mesh.

(1) Analyze the deformation mechanism of high-resistance steel wire mesh, deduce the relationship between in-plane deformability and shape parameters, define that the ratio of diameter and length of unit wall is the key factor to affect in-plane deformation of high-resistance steel wire mesh, make separately influence curves of $\beta$ and $\theta$ towards strain amplication coefficient and analyze their effect.

(2) Deduce separately relationships between elasticity modulus and $\beta$ and angle $\theta$, draw influence curves of $\beta$ and $\theta$ towards in-plane elasticity modulus and have the conclusion that is generally orthogonal anisotropic material (when angle $\theta = 45^0$, it's isotropy material); make comparison between theoretical equivalent elastic modulus obtained and results of test and FEM to verify the reasonability and correctness of in-plane mechanics property analysis of unit in this paper; study on out-of-plane vertical mechanical property of high-resistance steel wire mesh.

### Acknowledgements

The present research is funded by the National Natural Science Foundation of China (No. 51378495, No. 51408602), Chongqing Natural Science Foundation （NO.cstc2012jjB30004）and Graduate Students' Scientific Research Innovation Projects in Chongqing (No.CYB14102).

### References

Bertolo P., Oggeri C., Peila D., 2009, Full-scale Testing of Draped Nets for Rock Fall Protection. Can. Geotech. J., (46), 306-317. doi: 10.1139/T08-126

Daniel C.F., Luis L.Q, 2009, Design and Evaluation of Two Laboratory Tests for the Nets of a Flexible Anchored Slope Stabilization System. Geotechnical Testing Journal, 32(4), 1-10

Del Coz Díaz J.J., García Nieto P.J., 2009, Non-linear Analysis of Cable Networks by FEM and Experimental Validation. International Journal of Computer Mathematics, 86(2), 301-313. doi: 10.1080/00207160801965339

Gibson L.J., Ashby M.F., 1999, Cellular Solids : Structure and Properties (Second Edition). Cambridge University Press, England

He Y.M., Peng W., Yang Y.K., 2006, Typical Cases of Slope Flexible Protection System. Chinese Journal of Rock Mechanics and Engineering, 25(2), 323-328

Luo Y.M., Lei C.D., Zhou D.P., 2006, Discussion on Vegetation Methods and Stability of Slopes Reinforced by SNS Flexible stabilization system. Chinese Journal of Rock Mechanics and Engineering, 25(2), 235-240

Murray G., Gandhi F., Bakis C., 2010, Flexible Matrix Composite Skins for One-dimensional Wing Morphing. Journal of Intelligent Material Systems and Structures, 21(17), 1771-1781

Shi S.Q., Wang M., Peng X.Q., Yang Y.K., 2013, A new-type flexible rock-shed under the impact of rock block: initial experimental insights [J], Natural Hazards and Earth System Science, 13(12): 3329-3338. Doi: 10.5194/nhess-13-3329-2013

Shi S.Q., Wang M., Sun J.H., 2013, Experimental and Numerical Study on Anchored Cable Nets, Journal of Wuhan University of Technology, 35(10), 106-109

Wang M., Shi S.Q., Yang Y.K., 2014, Numerical simulation on flexible rock-shed under the impact of rockfall. Engineering Mechanics, 31(5), 151-157

Wang M., Shi S.Q., 2011, Numerical and Theoretical Analysis of Dissipation Energy Capacity of Ring Net Impacted by Rockfall, Journal of Vibration and Shock, 30(3), 10-12

Xiang B., He S.M., Ouyang C.J., 2014, Study About the Flexible Protection Technology Against Rockfall for the Deck of Shaping Bridge on the Dujiangyan-Wenchuan Highway. Journal of Sichuan University (Engineering Science Edition), 46(2), 8-13

Yang T., Zhou D.P., 2006, Stakility Evaluation of Slope Protected by Flexible System, Chinese Journal of Rock Mechanics and Engineering, 25(2), 294-298

Yang Y.K., Zhou Y.Q., Jiang R.Q., 2005, the Theory and Practice of Flexible Protection for the Geological Hazard of Slope. Science Press, Beijing

Yang Y.K., 2006, Concepts and Method of Slope Flexible Stabilization System. Chinese Journal of Rock Mechanics and Engineering, 25(2), 217-225

Zhang P., Zhou L., Qiu T., 2013, Mechanical Property Analysis and Structural Design of Flexible Skin Based on Deformable Honeycomb. Chinese Journal of Solid Mechanics, 34(5), 433-440